



OPEN

## Application of response surface methodology (RSM) for experimental optimization in biogenic silica extraction from rice husk and straw ash

Yigezu Temesgen Zewide<sup>1,2</sup>, Temesgen Atnafu Yemata<sup>1</sup>✉, Adane Adugna Ayalew<sup>1</sup>, Hawi Jihad Kedir<sup>1,3</sup>, Asab Alemneh Tadesse<sup>1,8</sup>, Asmarech Yeshaneh Fekad<sup>1,7</sup>, Alemayehu Keflu Shibesh<sup>1</sup>, Fentahun Adamu Getie<sup>6</sup>, Tegen Dagnew Tessema<sup>1</sup>, Tessera Alemneh Wubieneh<sup>4</sup>, Wondmagegn Wonago Kululo<sup>1</sup> & Muluken Tilahun Mihiret<sup>1,5</sup>

This work aimed to extract silica from combination of rice husk (RH) and Rice straw (RS) by optimizing the ash digesting process parameters with the aid of response surface methodology (RSM). The effects of three independent ash digestion process factors like sodium hydroxide concentration (1–3 M), temperature (60–120 °C) and time (1–3 h), for silica production from the mixture of rice husk (RH) and rice straw (RS) were studied. A quadratic model was used to correlate the interaction effects of the independent variables for maximum silica production at the optimum process parameters by employing central composite design (CCD) with RSM. The work indicates that the temperature is the most significant parameter among the model terms, followed by NaOH concentration, then time for digestion of ash for silica production. It may be because of the larger F-value for temperature, which influences to high extent of ash digestion for silica production. The proximate analysis discovered that RH/RS possessed compositions of high ash, volatile matter and fixed carbon content whereas low moisture content, i.e.,  $20.5 \pm 0.46$ ,  $67.1 \pm 0.78$ ,  $15.8 \pm 0.35$  and,  $6.6 \pm 0.37$  wt.%, correspondingly. The characterization of RH/RS and silica were performed by employing thermogravimetric (TG) and differential thermal (DT), Fourier transforms infrared spectroscopy (FTIR), X-ray fluorescence spectroscopy (XRF) and Brunner–Emmet–Teller (BET) for confirmation of the silica production. Hence, this current study concludes that silica materials obtained from RH/RS (with purity > 97.35 wt.%) may be new materials in the Si–C–O system that may be used in construction, ceramics and silica gel that helps to absorb moisture.

**Keywords** Rice husk, Rice straw, Optimization, Central composite design, Biogenic silica

Renewable materials like biomass contains inorganic and organic complex compound that is obtained from the agricultural, animal residues, plantation, and forestry<sup>1–4</sup>. Biomass has recently emerged as a promising class of renewable resource due to their distinct advantages such as no competition with land for foodstuffs and food production, no emission of hazardous materials in its utilization, fast-growing characteristic, abundant availability, and low economic value<sup>1,3,5–7</sup>. Renewable energy from biomass is one of the most promising energy sources and its use has been increased in the world. Many countries harvest large quantities of agroforestry waste

<sup>1</sup>Department of Chemical Engineering, Bahir Dar Institute of Technology, Bahir Dar University, P.O. Box 26, Bahir Dar, Ethiopia. <sup>2</sup>Department of Chemical Engineering, Dire Dawa University, P.O. Box 1362, Dire Dawa, Ethiopia.

<sup>3</sup>Department of Chemistry, Arba Minch University, P.O. Box 21, Arba Minch, Ethiopia. <sup>4</sup>Department of Materials Science and Engineering, Bahir Dar Institute of Technology, Bahir Dar University, P.O. Box 26, Bahir Dar, Ethiopia.

<sup>5</sup>Department of Chemical Engineering, University of Gondar, P.O. Box. 196, Gondar, Ethiopia. <sup>6</sup>Department of Chemistry, College of Natural and Computational Science, Injibara University, P.O. Box 40, Injibara, Ethiopia.

<sup>7</sup>Ethiopian Institute of Agricultural Research, National Agricultural Biotechnology Research Center, P.O. Box 249, Holeta, Ethiopia. <sup>8</sup>Ethiopian Institute of Agricultural Research, P.O. Box 249, Addis Ababa, Ethiopia. ✉email: atnafutemesgen16@gmail.com; e0012468@u.nus.edu

and utmost of which is contained of biomass that can be employed as fuel to get thermal and electrical energy. Hence, the conversion of agroforestry waste into energy can decrease the environmental impact of its disposal and enhance the value of the waste<sup>8–10</sup>. This waste is an outstanding biological source for various products, for instance animal feed, bioethanol, biogenic silica, biochar, and cellulose<sup>9,10</sup>. Since each of this waste possesses its composition, the end co-product (*i.e.* the ash) differs according to the physical and chemical properties of the biomass and the kind of it undergoes combustion as well<sup>11</sup>.

Due to the growing demand for silicate compounds and silica in construction materials, electronic devices, pigments, catalysts, drug delivery systems or pharmaceutical drugs, polymer nanocomposites, sensors and thermal insulators<sup>12,13</sup>, the need to develop new production methods has been increased. Hence, waste obtained from agricultural substrates becomes the most sustainable and cheapest sources for the manufacture of silica<sup>5,9</sup>. These wastes possess large silica content and can be employed for large-scale manufacture because of the cheap cost of the raw material and the silica quality attained<sup>5,9</sup>. Silicon has a protective function in plants that concentrate in the husks and it is picked up from the soil during the growth of the plant and its compound solubility is a result of temperature, soil pH and presence of bacteria<sup>14–16</sup>. Silicon dioxide ( $\text{SiO}_2$ ) or conventionally known as silica is one of the essential materials in the world<sup>17</sup>. It can present in many amorphous and crystalline forms and exists in different technological uses associated with its unique optical, electrical, mechanical, and piezoelectric properties<sup>18</sup>. Biogenic silica (bio-silica), *i.e.* bio-precursor, is an outstanding substitute to synthetic silica because of its density, structure, and variable composition<sup>9</sup>.

Raw materials particularly obtained from agricultural byproduct like rice husk and rice straw can substitute the conventional and expensive silica production<sup>19,20</sup>. Rice husk (RH) and rice straw (RS) are the two major agricultural by products available during rice production. Rice is a cereal grain that plays a critical role in the food and nutrition security for world nations. Besides its food security rice can generate a large amount of husk and straw. Rice husk and straw can generate waste if they are not properly disposed of or managed. Rice husk and rice straw are not recommended as livestock feed because of their low nutrient value. However, they are used for heat generation in boilers and as fuel in rural areas. After being used as fuel, they generate ash, which is often disposed of improperly, creating environmental challenges such as fly ash, which contributes to air pollution. However, this waste contains valuable material. The chemical composition of RH and RS is similar to that of other lignocellulosic resource and largely made of structural carbohydrates (cellulose and hemicellulose) and lignin. RH has cellulose, hemicellulose and lignin occupied from 28.6–43.3%, 18–43% and 18–43%, respectively and also has varying ash consists of 17–20%, whereas the cellulose, hemicellulose, lignin and ash content of RS can vary between 32.0–38.6%, 19.7–35.7%, 13.5–22.3% and 10–17%, correspondingly<sup>21,22</sup>. However, RH and RS possess high contents of silica in spite of most residue of crops<sup>23</sup>. The largest silica content in rice belonged to the husk. Ash content of RH and RS is between 10 and 20%<sup>21,22</sup>, and their ash possesses an approximate silica ( $\text{SiO}_2$ ) content of 75–95% in a hydrated amorphous form like silica gel<sup>23</sup>. Many researchers presented that the rice husk (RH) treated by thermal method can be converted into high-purity silica<sup>6,24,25</sup>, valuable carbon-based materials<sup>26</sup>, and other ceramic compounds (*e.g.* nitride and silicon carbide)<sup>27–29</sup>. For instance, Halimah et al. (2019) reported the  $\text{SiO}_2$  extraction with high purity from RH by using the cold acid leaching approach<sup>30</sup>. Beidaghy Dizaji et al. (2019) also investigated the utilization of RH and RS as renewable energy materials for the production of high-grade biogenic silica. They pointed out that combustion for a longer time and higher temperatures can enhance the silica purity up to 97 wt.%<sup>5</sup>. Recently, Khoshnood Motagh, et al. (2022) used RH and RS as the substrate for parallel silica and activated carbon production. They pointed out that the most vital superiority of RH to RS was its higher silica extraction yield from the initial biochar<sup>31</sup>.

Nevertheless, the proper use of rice waste (*i.e.* RH and RS) as a silica feedstock is still required. In reality, using RH and RS as the silica substrate will be useful not only for environmental aspect but also for economical point of view<sup>32–35</sup>. Even though several research works have been carried out on silica production from rice husk and straw ashes<sup>5,23,32,33,36–47</sup>, the synergic effect of hybrid RH/RS due to the different ash content and optimization of the ash digesting process variables by mixing with sodium hydroxide concentration (NaOH) solution for extraction of high-quality biogenic silica from RH/RS have not yet been investigated in detail. Hence, different from previous reports, our study employed response surface method (RSM) to optimize the ash digesting process variables including NaOH concentration (1–3 M), temperature (60–120 °C) and time (1–3 h.) and to study a synergistic effect between RH/RS by blending with NaOH solution in the extraction of silica form RH/RS material. RSM encompasses statistical and mathematical techniques that are vital for optimization (needs less experiment runs) and studying the interaction between the variables and can handle various variables at the same time as well<sup>48–50</sup>. Central composite design (CCD) was employed for extraction silica from RH and RS as the method is more efficient and practical design which is ideal for consecutive experimentation<sup>51</sup>. The results of this work reveal that hybrid RH/RS as a promising raw material for biogenic silica production that could be employed in construction, ceramics, pharmaceutical industry and cosmetic and production of nanosilicate materials as well.

## Experimental method

### Raw materials

The plant raw materials (*i.e.* RH and RS) were collected at Fogera Woreda, South Gondar in Ethiopia. Sodium hydroxide pellets (NaOH, 99.8%, Norbright, China), potassium bromide (KBr pellets, Merck, India) and hydrochloric acid (HCL, 37%, India) were found from local distributors/suppliers. All the chemicals employed were analytical grade and employed as received without any further purification. Distilled (DI) water was employed throughout the extraction of silica.

### Raw material preparation

At first, the RH and RS were washed with water to remove dust, sand and other particles. Then it was dried in oven at 110 °C for 12 h. to remove water<sup>52</sup>. Subsequent, RH and RS were ground using a grinding mill and the sample was passed through 2 mm mesh size sieve (AS PER IS: 460) and particles no < 2 mm in size were employed in for the extraction of silica in our experiments<sup>53</sup>. Then, few preliminary experiments were performed with varying the mixture of RH (%) and RS (%). Based the trial laboratory results, the mixture of 70 wt.% of RH and 30 wt.% RS, which resulted in high ash content, was selected for the current work. Moreover, in the present study, RH/RS has been used standing for 70 wt.% of RH and 30 wt.% RS hybrids. The complete pictorial illustration showing step-by-step experimental procedures in silica production from RH/RS ash is provided in Fig. 1. Furthermore, all the experiments were performed in triplicate, and the average analysis results of the data were provided.

### Silica extraction by sol-gelling process

#### Acid pretreatment

It was carried out to remove alkali, alkali earth metal and transition metal impurities such as K, Na, Ca, Mg, Al, Fe etc. from the RH/RS material. These metals can decrease the final purity of the silica yield such as porosity, colour and specific surface area. Acid leaching is important to produce the ash which is free from organic and carbonaceous matter during combustion process. Leaching the sample with 1 M of HCl yields high quality silica<sup>52,54</sup>. The RH/RS sample was taken in to a beaker that contains 1N HCl solution of 500 ml and then heated with hot plate at temperature of 90 °C for 2 h (hrs.) under constant stirring with a magnetic stirrer at 500 rpm. Subsequently the leached material was filtered in a paper filter and then washed with DI water many times until the pH of the solution recorded up to 7<sup>55</sup>. Finally, the acid treated solid material was put inside the oven and dried at temperature of 110 °C for 12 h. before the calcinations process.

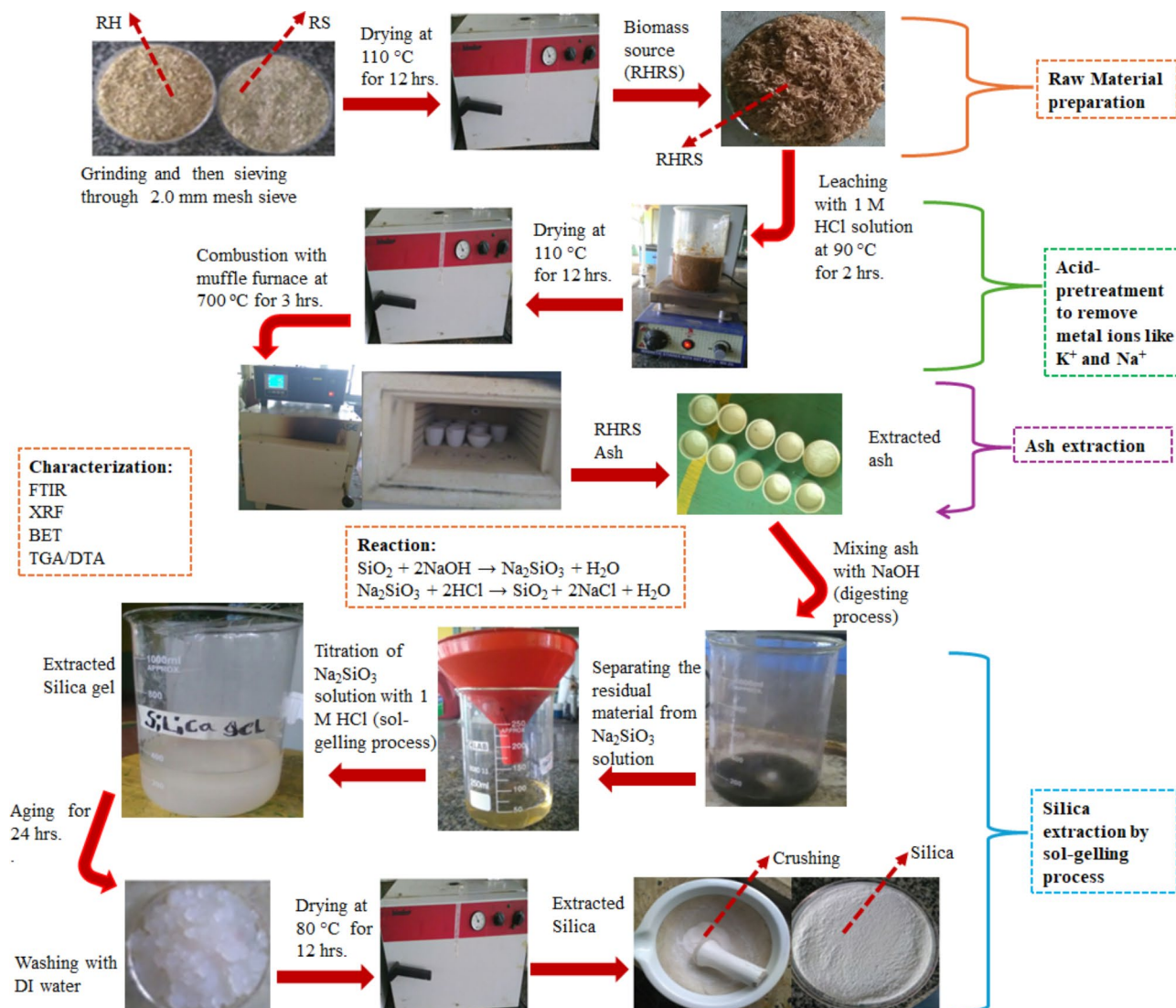


**Fig. 1.** Schematic flow chart illustrates the step-by-step procedure to extract silica from RH/RS.

*Ash production*

The pre-oven dried acid leached material was calcinated in a muffle furnace at temperature of 700 °C for 3 h. in the presence of air<sup>41</sup>. After calcination cycles, the recovered ashes were labelled and put inside a desiccator.

*Ash digestion of RH/RS in NaOH*

The resulting RH/RS ash was then mixed with NaOH (digesting process) and kept at 500 rpm (constant agitation) to create sodium silicate ( $\text{Na}_2\text{SiO}_3$ ) solution (Eq. 1). The approach adopted is essentially showed by Falk et al.<sup>42</sup>. Next, the mixture was filtered in filter paper and then the filtered  $\text{Na}_2\text{SiO}_3$  solution was allowed to cool to room temperature. The digestion process was done by using 1:10 solid/liquid (g/ml) ratio<sup>36,57</sup>.

*Response surface method (RSM)*

In this study, central composite design (CCD) was employed by using the Design-Expert 7.1 software (trial version). RSM that consists of statistical and mathematical techniques are vital for modelling and analysing problems in which the response is determined by numerous factors. The main objective of the response surface is to attain an optimize response factors<sup>48–50</sup>. RSM was used to optimize the ash digestion process variables in NaOH for extraction of silica from the RH/RS. Here, the central composite design (CCD) from RSM, which is more practical than other approaches, was employed to optimize and study the interaction effects of ash digestion process variables namely NaOH concentration, digestion temperature and digestion time. The range of the parameters is presented in Table 1. Here, few trial experiments were performed to identify the ranges of the ash digesting parameters. These trials results are consistent with results from previous study reported somewhere else<sup>56,57</sup>. To model the influence of these parameters on the extracted silica yield, 20 experiments were generated using CCD. The results were analysed using ANOVA with the aid of Design Expert version 7.1 software.

In the process optimizing, the response can be directly related to selected factors by quadratic or linear models. A quadratic model (Eq. 2)<sup>58–66</sup> is the appropriate model since there are only three levels for each factor.

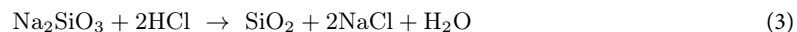
$$Y = \beta_0 + \sum_{i=1}^{k=3} X_i \beta_i + \sum_{i=1}^{k=3} X_i^2 \beta_{ii} + \sum_{i=1}^2 \sum_{j=i+1}^{k=3} X_i X_j \beta_{ij} + e_i \quad (2)$$

where  $\beta_0$  is a coefficient (constant);  $X_j$  and  $X_i$  are the factors;  $Y$  is the response;  $\beta_{ii}$ ,  $\beta_{ij}$ , and  $\beta_i$  are the coefficients (interaction) of quadratic, second-order and linear terms, correspondingly;  $k$  is the number of examined factors and;  $e_i$  is the error<sup>60,63,67–70</sup>. These variables were selected according to the preliminary experimental results as the critical parameters nominated as  $X_1$ ,  $X_2$ , and  $X_3$ .

The correlation coefficient,  $R^2$ , was employed to scrutinise the fit of the quality of model (*i.e.* polynomial). The probability value (Prob > F) and the model adequate precision and Fisher variation ratio (F-value) as well are the crucial indicators that validate the significance and adequacy of the used model<sup>48,59,60,71</sup>.

*Sol-gelling process*

Subsequently, the resulting solution was titrated with 1 M HCl (sol-gelling process, Eq. (3)) under constant stirring 600 rpm until the pH of the solution reached 7<sup>42</sup>.



Then after 24 h. of ageing time, the silica gel was easily cracked and firstly washed with DI water. The filtered gel was washed with DI water for several times until free of sodium chloride (NaCl) and then dried in the oven at 110 °C for 12 h. Finally, the resulting gel was crushed in a pestle and agate mortar and stored in a vacuum desiccator for further characterization<sup>32,40,42</sup>. The yield of extracted silica from RH/RS was calculated according to Eq. (4). The employed approach is basically demonstrated by previous studies presented somewhere else<sup>40,72</sup>.

$$\text{Percent yield of silica (\%)} = \frac{\text{Mass of extracted silica (g)}}{\text{Mass of ash (g)}} \times 100 \quad (4)$$

Parameters	Unit	Levels	
		Low (-1)	High (+)
NaOH concentration; A	M	1	3
Temperature; B	°C	60	120
Time; C	hr	1	3

**Table 1.** Independent parameter ranges for the RSM designs.

## Characterization

Proximate analysis of biomass sample estimates volatile matter (VM), moisture, ash and fixed carbon (FC) content in a fuel material as described by the American Society for Testing and Materials (ASTM) standards<sup>73,74</sup>. Though originally established for coal sample, proximate analysis has been acquired for different solid fuels and biomass as well<sup>74,75</sup>. The proximate analysis was estimated based on the approach reported by Racero-Galaraga et al.<sup>[74]</sup> and Hosseinpour et al.<sup>75</sup>. The thermogravimetric (TG) and differential thermal (DT) analysis of RH/RS were conducted on a BJHENVEN HCT-1 instrument. Fourier transform infrared spectroscopy (FTIR, Model Jasco-6600, Japan) was employed to identify the functional groups in the sample by creating an infrared absorption spectrum. The RH/RS material and extracted silica spectra were obtained with wavelength range of between 4000–500  $\text{cm}^{-1}$  regions by employing a spectrometer with a detector at 4  $\text{cm}^{-1}$  resolution and 25 scan rates. X-ray fluorescence spectroscopy (Siemens Model SRS 3000, XRF) was employed for determination of silica ( $\text{SiO}_2$ ) content and other chemical impurities exist in the extracted silica materials. The Surface area and pore volume of the extracted sample were conducted by using Brunner-Emmet-Teller (BET) (Quanta chrome Instruments, version 11.0, Quanta chrome Nova Win model).

## Results and discussion

### Proximate analysis of RH/RS

The proximate analysis results of the raw material (*i.e.* RH/RS) are presented in Table 2. The results were consistent with the previous studies reported somewhere else<sup>76–87</sup>. The proximate analysis of biomass comprises vital variables like ash, moisture, fixed carbon, and volatile matter, all of these are essential for evaluating its viability of energy<sup>74</sup>. Moisture affects combustion efficiency, as high moisture content lowers the calorific value by requiring additional energy to evaporate the water before effective combustion can occur<sup>74</sup>. The moisture content of RH/RS sample was found to be 6.6 (wt. %) (Table 2), which was in agreement with the previous studies<sup>76,77</sup>. Ash, final inorganic residue substance after the combustion of biomass is, which is a standard measurement for solid fuels<sup>74,88</sup>. The ash analysis result showed that an average ash content of 20.5 wt.% was obtained for RH/RS material (Table 2), indicating a high percentage value of ash yield due to the synergistic effects between RH and RS, that will result in highest yield of silica. This result is basically matched with the previous studies<sup>83–85</sup>. VM, which comprises of the gases released through the beginning steps of combustion, helps in combustion stability and fuel ignition<sup>74,89,90</sup>. The VM values obtained for RH/RS ( $67.1 \pm 0.78$  wt.%, Table 2) is in agreement the previously reported results<sup>78,79</sup>. Moreover, FC, indicates the portion of carbon content remaining after volatiles and moisture have been expelled, is related to the calorific value and aids as a main indicator for the energy potential's of biomass<sup>74,91</sup>. The FC was estimated based on the ASTM Standard D 3172–89 by subtracting the moisture, VM, and ash content from the initial biomass weight (*i.e.* FC, wt.% = 100 – (ash, wt.% + moisture, wt.% + VM, wt.%))<sup>92</sup>. The FC values found in this work ( $5.8 \pm 0.35$  wt.%) is different from the previous result (11.1 wt.%)<sup>86,87</sup>. This difference could be due to the kind of rice, geographical-linked condition, climate, and planting time<sup>54</sup>. Lastly, biomass basically possesses a VM/FC ratio of  $> 4.0$ <sup>93,94</sup>. In this study, the VM/FC ratio for the RH/RS material is about 11.6, indicating the main form of combustion will occur through the volatile species gas-phase oxidation<sup>93,95</sup>.

### TG and DT analysis of RH/RS

TG/DT analysis was employed to examine the presence of organic constitutes in the RH/RS. (Fig. 2). 10 mg of sample was kept in corundum crucible and then heated up to a 700  $^{\circ}\text{C}$  temperature at 20  $^{\circ}\text{C}$  per minute heating rate in the air atmosphere. It can be observed that four temperature stages have been obtained. The first stage (80–220  $^{\circ}\text{C}$ ) demonstrated that the mass loss happened at temperature between 80–220  $^{\circ}\text{C}$ . This can be due to the loss of adsorbed moisture and other volatile components<sup>96,97</sup>. The loss of these components was verified by the discovery of the same temperature for TGA and DTA profile at  $< 175$   $^{\circ}\text{C}$ .

The second stage indicated a large mass reduction within 200–350  $^{\circ}\text{C}$ . This mass reduction occurred because of the thermal degradation of hemicellulose and cellulose as main organic constituent in the RHRS<sup>96–99</sup>. This is verified by the occurrence of exothermic peak at approximately 345  $^{\circ}\text{C}$  in the DTA analysis.

The third stage (between 380–585  $^{\circ}\text{C}$ ) revealed the mass loss which was owing to degradation of lignin<sup>96–98</sup>. This was verified by the discovery of exothermic peak at about 485  $^{\circ}\text{C}$  in the DTA plot.

In the fourth stage ( $> 590$   $^{\circ}\text{C}$ ), no mass reduction was detected<sup>97,98</sup>. The degradation rates are no longer significant and no mass loss detected as all volatile organic constituents were converted entirely. The ash residual is mostly the silica (non-combustible)<sup>97</sup>.

The TGA/DTA results demonstrated that the heat treatment, can eradicate organic constituents, is crucial to be performed prior to silica production process<sup>32,47,97,100</sup>.

Proximate analysis variables	Current study	References
Ash	$20.5 \pm 0.46$	<a href="#">83–85</a>
Moisture	$6.6 \pm 0.37$	<a href="#">76,77</a>
VM	$67.1 \pm 0.78$	<a href="#">78,79</a>
FC	$5.8 \pm 0.35$	<a href="#">86,87</a>

**Table 2.** Proximate analysis results of RH/RS material (dry basis, wt.%).

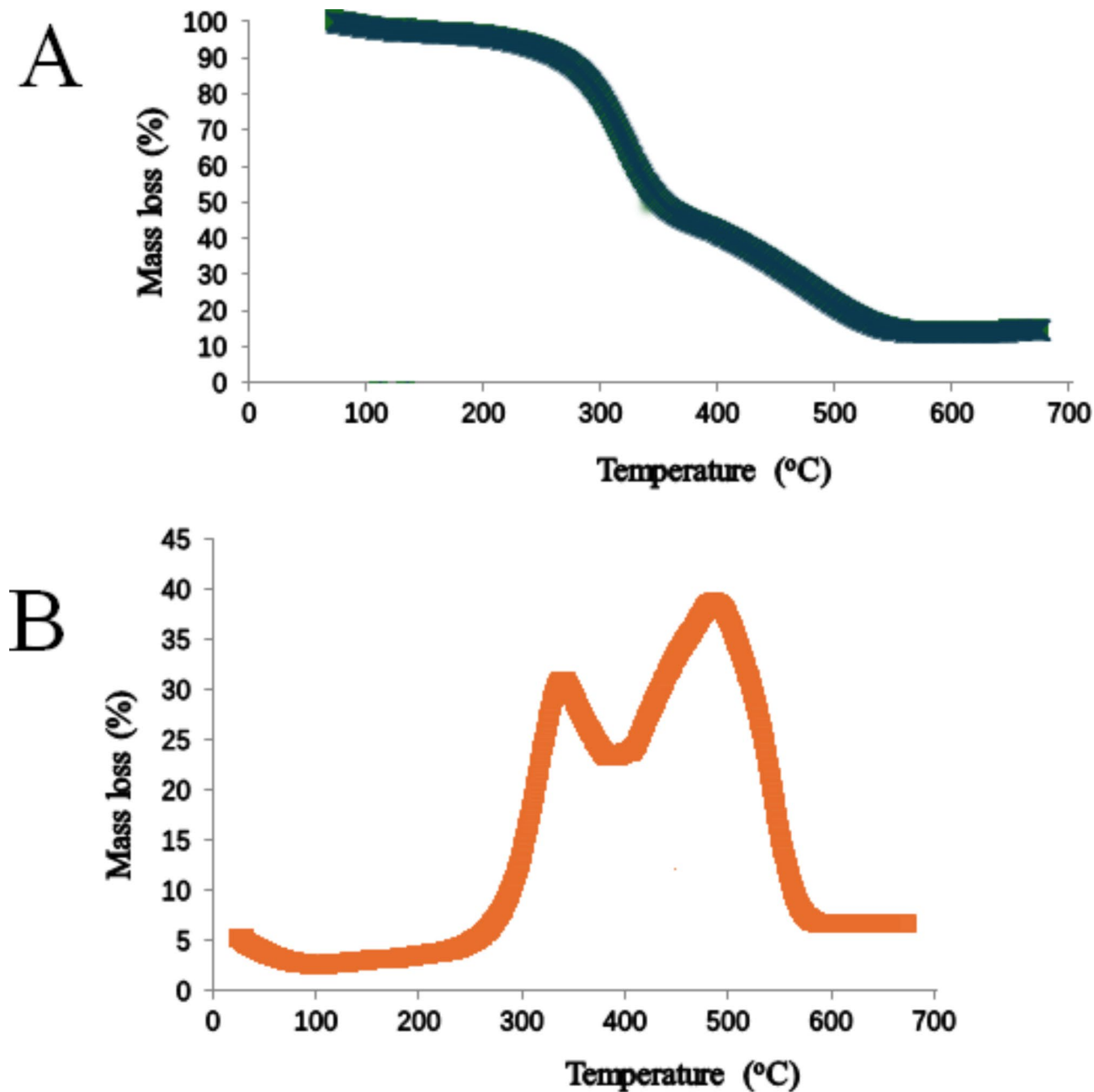


**Fig. 2.** Thermogravimetric (TG) and differential thermal (DT) plots of RH/RS.

#### Surface functional groups analysis using FTIR

Figure 3 shows the FTIR spectra of the raw RH/RS material and the extracted silica. For both samples, the peaks about 1100 and 870 were assigned to CHOH and Si–O–Si stretching correspondingly while the peak around 618 cm<sup>-1</sup> ascribed to Si–H groups<sup>97,101–103</sup>. Also, these two samples possessed peaks at 1000, 700 and 450, in which these peaks were ascribed to Si–O–Si asymmetric stretching, Si–O–Si symmetric stretching and Si–O–Si stretching, correspondingly (Fig. 3). However, for RH/RS, we obtained a peak which was not attained in the silica. For instance, in the FTIR spectra of RH/RS (black, Fig. 3), the peak about 3250 cm<sup>-1</sup> showed the presence of free OH groups. The RH/RS bands around 1600–1750 cm<sup>-1</sup> assigned to the stretching of C=O that may be ascribed to the aromatic groups of lignin and hemicelluloses<sup>104,105</sup>. The C=C stretching vibrations of RH/RS around 1500–1600 cm<sup>-1</sup> showed the alkenes and aromatic functional groups and the peak around 1383 cm<sup>-1</sup> and 1250 cm<sup>-1</sup> were ascribed to the presence of CH<sub>2</sub> and CH<sub>3</sub><sup>102,105</sup>. Similarly, in the FTIR spectra of the extracted silica (Fig. 3 (red), different from RH/RS, the bands around 500 and 1000 cm<sup>-1</sup> assigned to the O–Si–O symmetrical stretching vibrations which is similar with the previous findings<sup>106,107</sup>. Moreover, the spectra between 1000 and 1500 cm<sup>-1</sup> indicated the existence of O–Si–O vibration in extracted silica that attributed to the vibration of asymmetrical stretching bands which is identical to the study reported somewhere

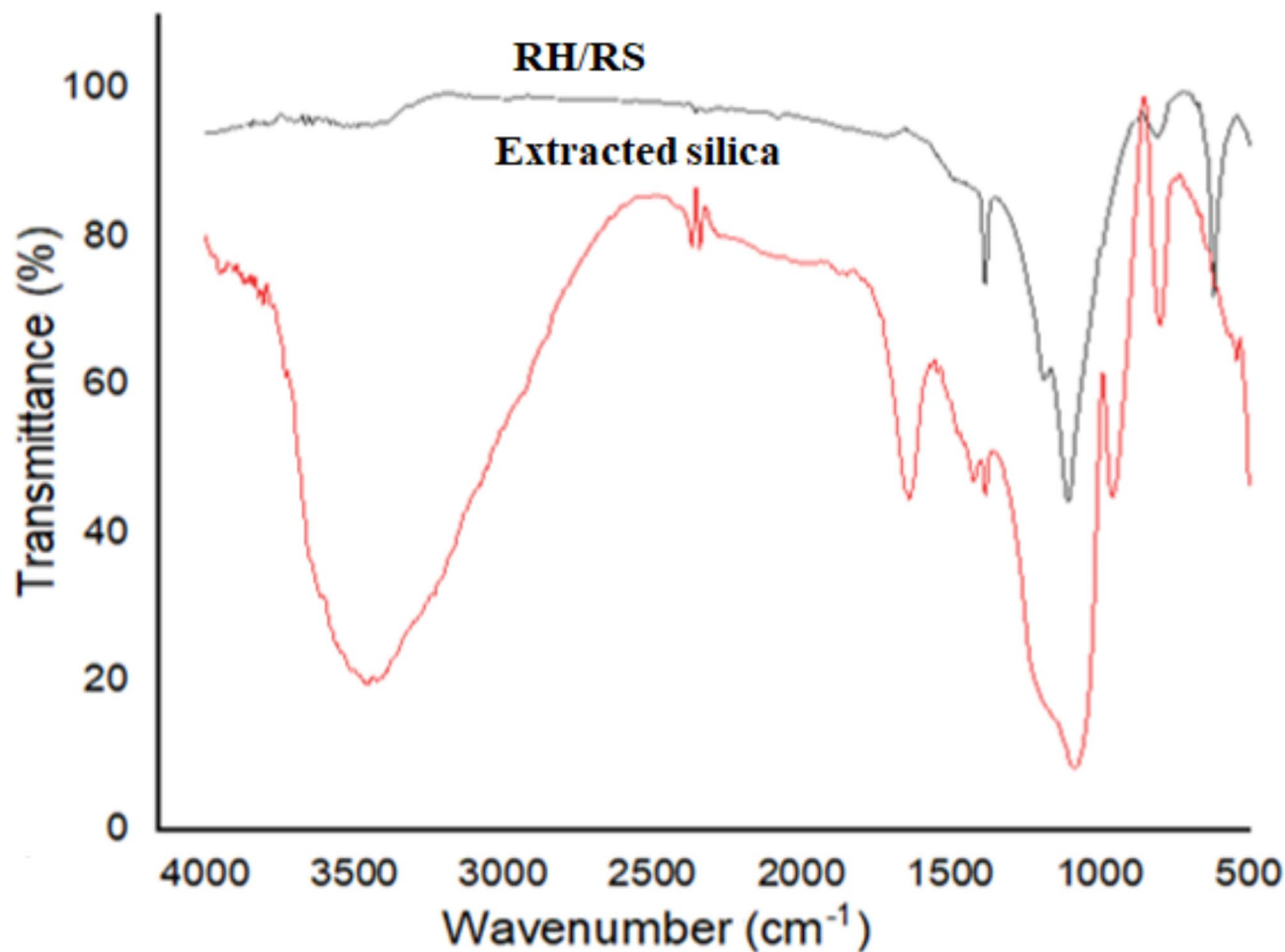


**Fig. 3.** FTIR spectra of raw RH/RS (black) and extracted silica (red).

No	Compositions, wt.%	Extracted silica at the optimized conditions
1	SiO <sub>2</sub>	98.74
2	Al <sub>2</sub> O <sub>3</sub>	0.26
3	CaO	0.23
4	Fe <sub>2</sub> O <sub>3</sub>	0.18
5	P <sub>2</sub> O <sub>5</sub>	0.16
6	SO <sub>3</sub>	0.13
7	Cl	0.11
8	ZnO	0.08
9	Na <sub>2</sub> O	0.05
10	MgO	0.03
11	K <sub>2</sub> O	0.02
12	MnO	0.01

**Table 3.** Chemical constituents of extracted silica.

else<sup>108</sup>. Furthermore, for silica, the bands around 3550 and 3750 cm<sup>-1</sup> assigned to the free water band because of the H<sub>2</sub>O molecules stretching vibration<sup>109</sup>. This result also agreed with the previous works<sup>108,110</sup>. Finally, the peak for extracted silica detected between 550 and 700 cm<sup>-1</sup> demonstrated the formation of crystalline, what typically noticed as crystalline silica<sup>108,111</sup>.

#### XRF analysis

XRF was employed to identify the purity and chemical compositions of silica extracted from the RH/RS (Table 3). To verify the composition and purity, XRF was performed for extracted silica at the optimized ash digesting

Optimum variables				Silica yield (wt.%)		
Solution no	A (M)	B (°C)	C (hrs.)	Experimental value	Predicted value	Desirability
1	2.07	95.42	2.78	97.35	97.40	1

**Table 4.** Optimization results derived by CCD for silica yield.

Parameter	Extracted silica
BET surface area (m <sup>2</sup> /g)	225
Total pore volume (cm <sup>3</sup> /g)	0.41
Pore diameter (Å)	58.61

**Table 5.** BET surface area of extracted silica.

process conditions as a proof for laboratory result. The XRF result showed that silica ( $\text{SiO}_2$ ) content was 98.74 wt.% purity. This higher value (98.74 wt.%) was attributed to the decrease in the impurities (*i.e.* other metal oxides) due to the acid leaching during sol-gelling process<sup>97</sup>, which fitted well with the experimental value (*i.e.*, 97.35 wt.%, optimized value obtained from Table 4). The values are in good agreement with other studies reported elsewhere<sup>31,42,97,112–114</sup>. This result demonstrates that the RH/Rs is one of the promising materials for biogenic silica resources.

### Surface area and porosity

Table 5 presents the BET surface area, pore diameter and total pore volume of extracted silica.

According to Table 5, the extracted silica possessed a BET surface area of 225 m<sup>2</sup>/g and pore volume of 0.41 (cm<sup>3</sup>/g). The higher pore volume and surface area values are largely ascribed to the effect of acid (HCl) leaching treatment that resulted in the hydrolysis of cellulose and hemicellulose into smaller components which might degrade easier in combustion process<sup>97</sup>. The smaller average pore diameter of silica (about 58.61 Å) indicated that acid leaching treatment resulted in reduced pore diameter. The surface area value obtained is in agreement with the result obtained by Bakar et al.<sup>97</sup> and Mahmud et al.<sup>114</sup>.

### Model development and statistical analysis

In this study, the Design-Expert 7.1 software (trial version) was employed to examine the experimental data regression analysis and to plot the response surface curves. In order to determine the influence of the factors and their interactions effect, the statistical variables have been estimated by employing Analysis of variance (ANOVA) in the optimal Central Composite Design (CCD) test<sup>48,59,60</sup>. The NaOH concentration ranged from 1 to 10 M, the temperature ranged from 60–120 °C and time 1 to 3 h, high (coded + 1) and low (coded – 1) set points, for ash digestion process variables have been selected according to the values achieved in preliminary tests. Table 6 presents the required experimental variables and ranges for-ash digestion process in NaOH in that have been employed in the current study. The experimental results of 20 runs of the design of experiments using CCD on three factors is shown in Table 6.

The experimental analysis of our results (Table 6) provides to mathematical relationship that convey silica yield as function of interaction and individual contribution of parameters (Eq. 5). Hence, in terms of a coded variables, the final regression model (second-order polynomial) for silica extraction (wt.%) is indicated in Eq. 5:

$$\text{Silica yield (wt. \%)} = +90.01 + 6.00 * A + 7.10 * B + 5.31 * C + 6.75 * A * B + 7.50 * A * C - 38.45 * A^2 \quad (5)$$

where the positive sign presents the synergistic effects and the negative sign shows the antagonistic effects.

The test for significance of the individual model and regression model coefficients with lack of fit test was conducted to fit a good model. Often, the significant variables have been ranked according to the P-value (probability value) or F-value with 95% confidence level. Table 7 presents the ANOVA of regression factors for the data obtained by using Eq. 5 for silica extraction from RH/Rs. The smaller 'P' value and the larger F-value (Prob. > F), indicate more significant of the model for corresponding coefficient<sup>35</sup>. The F-value of 21.74 revealed that the model is significant for silica yield. Moreover, the model terms are not significant only when the Prob. > F values of are > 0.1000 whereas values < 0.05 indicate the significant model terms<sup>115</sup>. In this case, A, B, C, AB and AC are significant model terms on response while interactional effects between BC, B<sup>2</sup> and C<sup>2</sup> are not significant model terms that had limited effect. These not significant terms were excluded in order to enhance the model.

The model adequate precision ratio of 12.319, which is > 4, revealed the adequacy of the signal model<sup>116</sup>. Thus, the model developed can be employed to guide the design space. The Lack of fit F- statistic value of 1.97 suggests that the Lack of fit is not significant since the P values is > 0.05 (Table 7). The non-significant lack of fit in Table 7 implies that the quadratic model is statistically significant and can be employed for further analysis. Furthermore, the multiple correlation coefficient ( $R^2$ ) value of 0.9514 was obtained for silica extraction, which is > 0.80, revealing that only 4.86% of the total variation might not be described by the empirical model. For a good fit of a model, the  $R^2$  should be at least 0.8 as described by Joglekar et al.<sup>117</sup>. The High  $R^2$  results reveals

Run	Variables			Silica yield (wt.%)	
	A	B	C	Observed*	Predicted**
1	1	90	2	44	45.56
2	2	90	3	96.2	90.01
3	3	60	1	40	33.95
4	2	60	2	70	79.96
5	3	90	2	50	57.56
6	2	90	2	95	90.01
7	1	60	1	50	50.45
8	3	120	1	50	51.65
9	1	60	3	40	36.07
10	2	90	2	93	96.32
11	3	120	3	90	87.27
12	2	90	2	96	90.01
13	3	60	3	50	49.57
14	2	120	2	95	94.16
15	1	120	1	43	41.15
16	2	90	1	79.9	85.70
17	2	90	2	81.1	90.01
18	2	90	2	95	90.01
19	1	120	3	43	46.77
20	2	90	2	95	90.01

**Table 6.** Experimental variables in actual and coded units and experimental response (silica yield) for the CCD. \*Experimental results of response. \*\*Predicted results of response by CCD proposed model.

Source of variation	Sum of square	DF	Mean square	F value	P value	Remarks
Model	10,033.25	9	1114.81	21.74	<0.0001	S
A	360.00	1	360.00	7.02	0.0243	S
B	504.10	1	504.10	9.83	0.0106	S
C	281.96	1	281.96	5.50	0.0410	S
AB	364.50	1	364.50	7.11	0.0236	S
AC	450.00	1	450.00	8.78	0.0142	S
BC	200.00	1	200.00	3.90	0.0765	NS
A <sup>2</sup>	4065.61	1	4065.61	79.30	<0.0001	S
B <sup>2</sup>	23.93	1	23.93	0.47	0.5100	NS
C <sup>2</sup>	2.75	1	2.75	0.054	0.8215	NS
Residual	512.69	10	51.27			
Lack of fit	339.85	5	67.97	1.97	0.2379	NS
Pure error	172.84	5	34.57			
Correlation total	10,545.94	19				

**Table 7.** ANOVA for analysis of variance and adequacy of the response surface quadratic model for silica extraction for CCD obtained by the Design Expert 7.1 software. Std. Dev. = 7.16; PRESS = 2957.34; R<sup>2</sup> = 0.9514; Adj R<sup>2</sup> = 0.9076; Adeq Precision = 12.319. DF- Degree of freedom; S- Significant; NS-Not significant.

good similarity between the actual and predicted values in the range of experiment. Similar results had been demonstrated and discussed elsewhere<sup>59,118</sup>.

In general, it is crucial to check the adequacy of real system approximation with the developed model in order to verify the data analysis of the experiment<sup>119</sup>. By employing the diagnostic plots, like studentized residuals versus normal probability plots, the adequacy of the model can be checked. The normal probability of studentized residual plot was presented in Fig. 4 for extraction of silica from RH/RS. It has been found from Fig. 4 that there was neither response transformation nor any apparent problem with normality. It can be found that there was a normal distribution of data (Fig. 4). The predicted silica yield and internally studentized residual is presented in Fig. 5. This indicates that the variance of original value is constant for the entire response values (*i.e.* the random scatter plot) and there was no need for response factors transformation. Figure 6 shows the actual versus the predicted percentage for silica extraction from RH/RS. It was discovered that the values of adjusted R<sup>2</sup> (Adj R<sup>2</sup>) and R<sup>2</sup> were 90% and 95% correspondingly. The result of R<sup>2</sup> indicated up to what level perfectly developed model

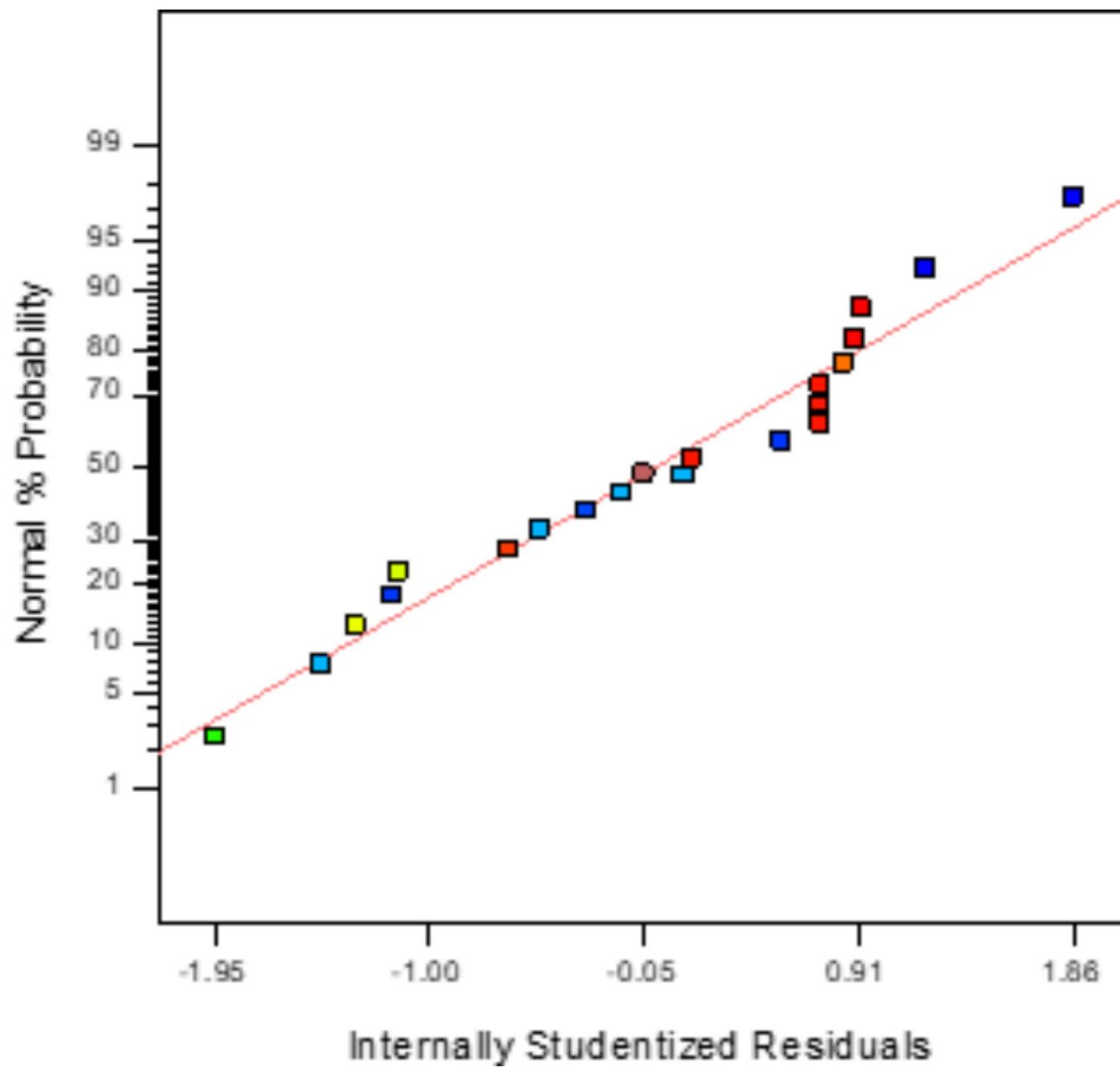


**Fig. 4.** Studentized residuals versus normal percentage probability plot for silica extraction.

can appraised the data points (experimental) and the value of adjusted  $R^2$  described the quantity of variation about mean described by the developed model. Thus, the model is found to be adequate. Similar results were shown and discussed by previous reports<sup>59,118,120–122</sup>.

#### Three-dimensional (3-D) response surface plots

The RSM assigned to CCD model was illustrated and examined to optimize the crucial variables and depict the response surface nature in the experiment<sup>59</sup>. Based on the ANOVA, the 3-D response plots were discovered according to the quadratic model from the combined effect of the three parameters on silica production from RH/RS. In each plot, as presented in Fig. 7, one variable was maintained constant while the other two factors were tested on silica yield in the experimental ranges. The combined effect of NaOH concentration (A) and temperature (B) on silica yield at constant time of 2 h. is demonstrated in Fig. 7A. It can be observed from the results, NaOH concentration (A) and temperature (B) had lower effects on silica extraction from HR/HS owing to the low result of F statistics. Similarly, Fig. 7B presents the combined effect of NaOH concentration (A) and time (C) on silica production form HR/HS at 90 °C (constant temperature). The results indicated that interaction between the NaOH concentration and time possessed higher effect in silica yield. Similar results with analogous situations and supposition had been presented and discussed somewhere else<sup>59,60,121,122</sup>.

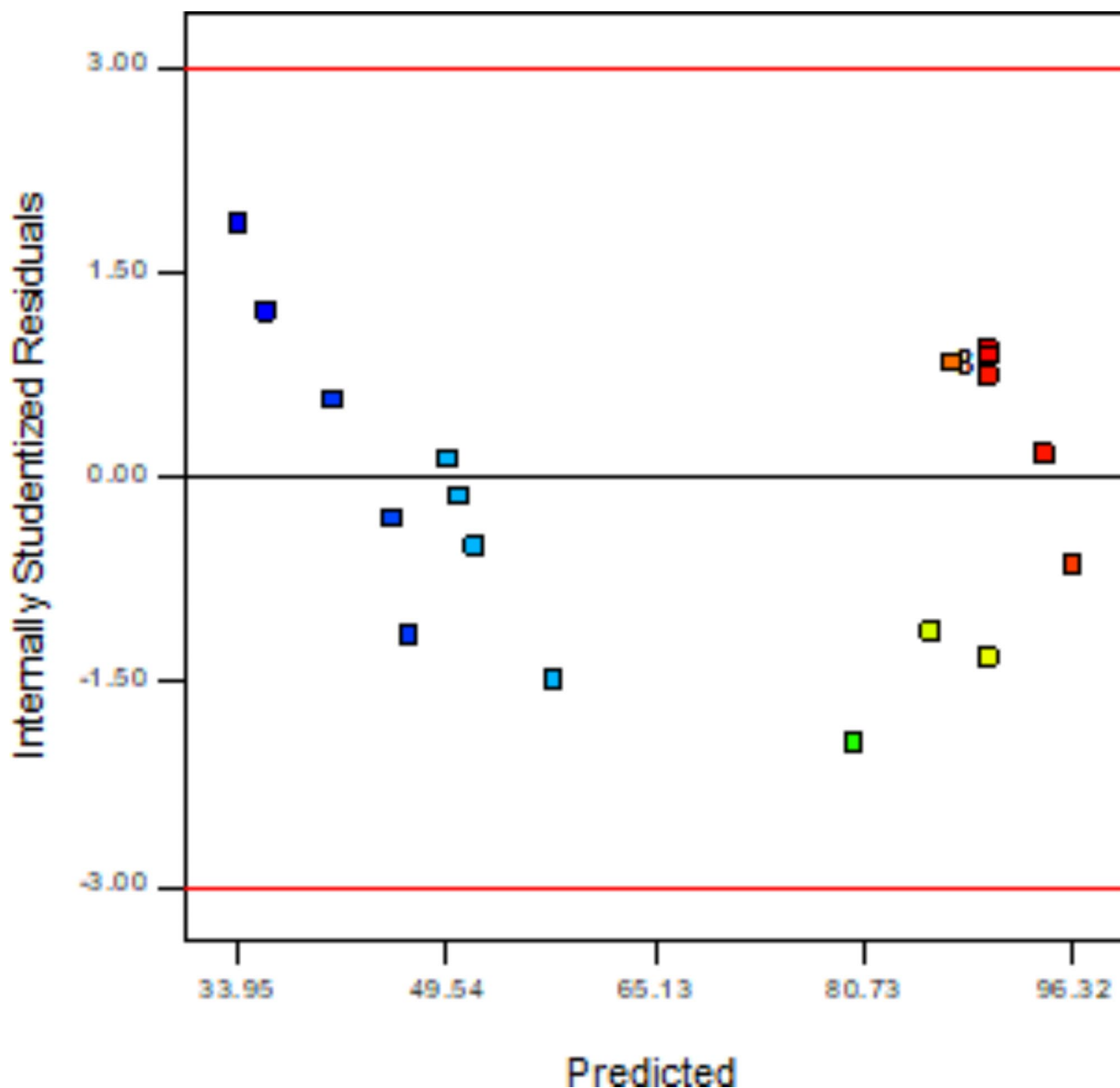


**Fig. 5.** Predicted silica extraction of RH/RS and studentized residuals plot.

#### Optimization of ash digesting process variables by RSM

Profiling the desirability option and the predicted values in the Design-Expert 7.1 software (trial version) was employed for process optimization. The profile of desirability responses comprises stating the function for desirability for the dependent factor (silica yield, wt.%) by allocating a score for predicted values ranging from 0 (very undesirable) to 1 (very desirable). Based on the desirability score of 1.0 (Table 4), silica extraction was optimized at 97.35 wt.% at optimized ash digesting parameters of 2.07 M NaOH, temperature (95.42 °C) and 2.78 h. of digestion time. For validation at these optimized ash digesting parameters, the experiment was performed in triplicate and the results revealed that there was <0.05% error between the actual (97.35 wt.%) and predicted (97.4 wt.%) values for the silica yield from RH/RS. The results were estimated and discussed on the bases of the analysis approached reported by Asfaram et al.<sup>59</sup> and Agarwal et al.<sup>60</sup>. Hence, the present research concluded that designed model could predict the relation between the variables and silica yield.

#### Conclusion

In this study, silica extraction from RH/RS was optimized using CCD with RSM. The effects of three independent ash digestion process variables including NaOH concentration (1–3 M), temperature (60–120 °C) and time (1–3 h.) using a quadratic model for maximum silica production. The present study demonstrates that the temperature is the most significant parameter among the model terms, followed by NaOH concentration, then

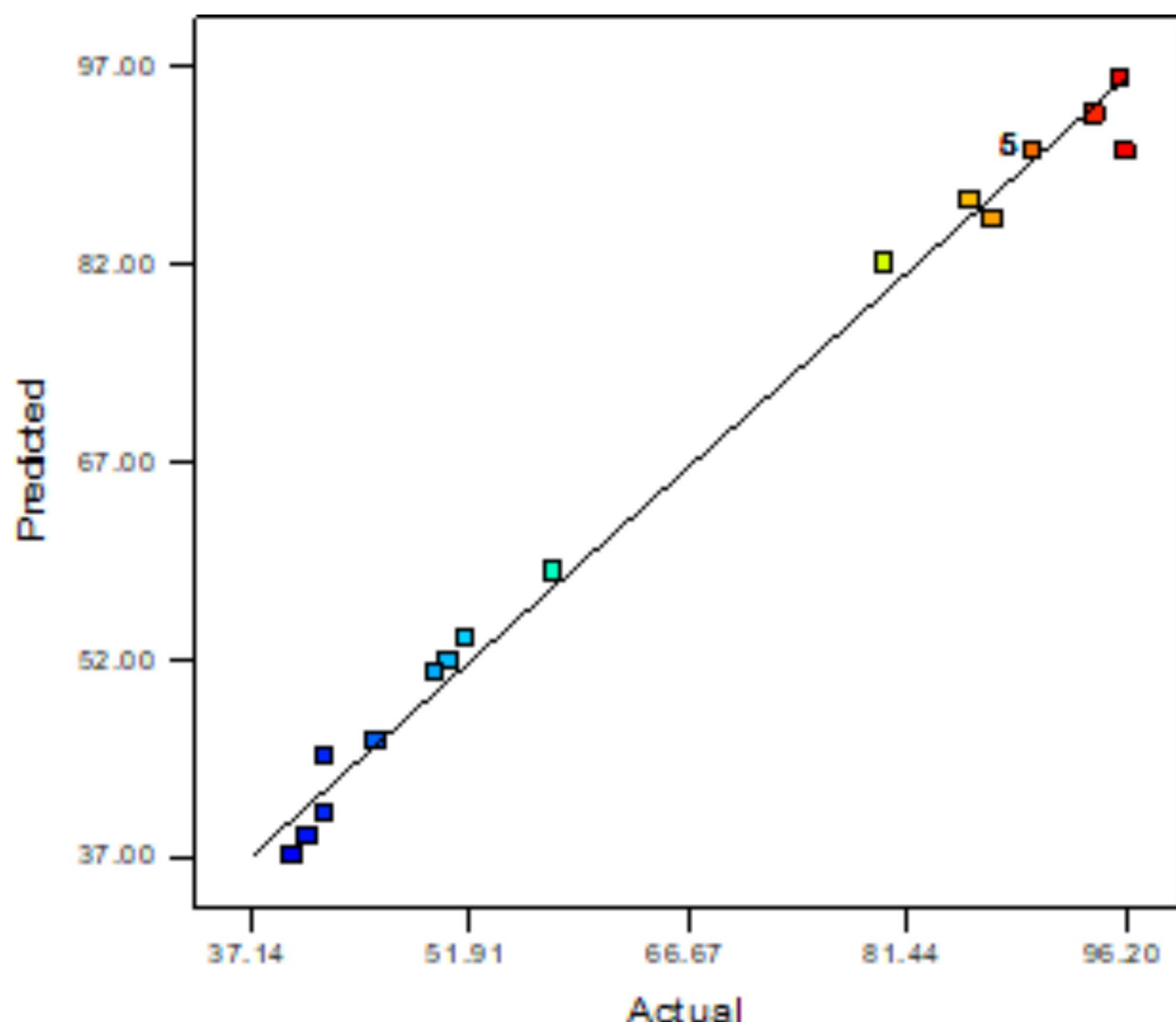


**Fig. 6.** The observed values (experimental data) versus predicted values for silica extraction.

time for digestion of ash for silica production. At the optimized ash digesting variables, the experimental and predicted values, for the silica yield from RH/RS were found as 97.35 wt.% and 97.4 wt.%, correspondingly, with error less than 0.05%. Hence, the results indicated that the model developed could precisely predict the silica extraction. The extracted silica can be a potential material in construction, ceramics and silica gel application.

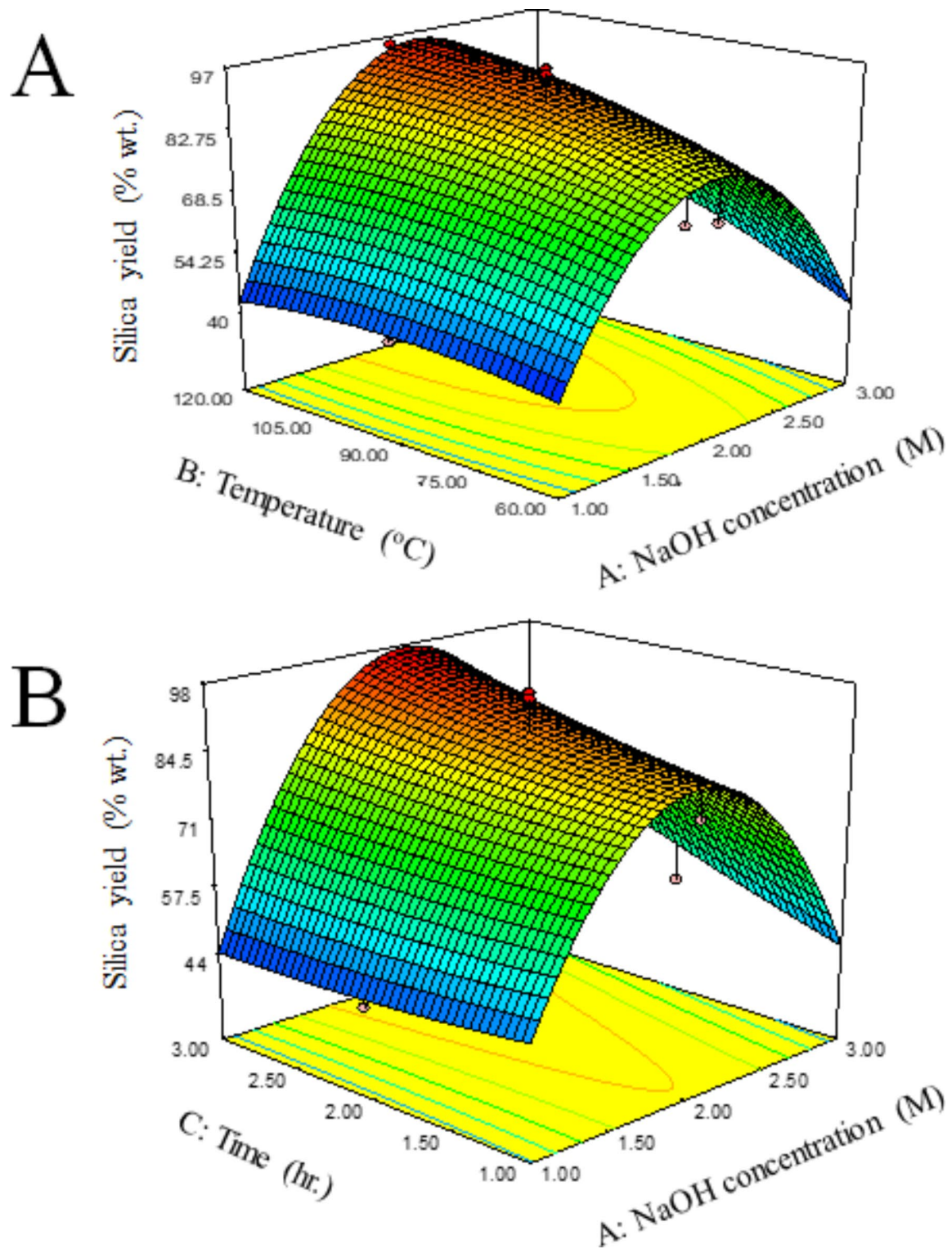


**Fig. 7.** Response surface plots for the CCD for silica extraction as a function of: (A) NaOH conc. and temperature (at time 2 h.) (B) NaOH conc. and time (at temperature 90 °C).

#### Data availability

The authors state that the data supporting the results of this work are available within the paper. The raw data can be provided from the corresponding author on reasonable request.

Received: 10 September 2024; Accepted: 17 December 2024

Published online: 02 January 2025

## References

1. Dessie, W. et al. Current advances on waste biomass transformation into value-added products. *Appl. Microbiol. Biotechnol.* **104**(11), 4757–4770 (2020).
2. Steven, S. et al. Routes for energy and bio-silica production from rice husk: A comprehensive review and emerging prospect. *Renew. Sustain. Energy Rev.* **149**, 111329 (2021).
3. Nunes, L., Matias, J. & Catalão, J. Mixed biomass pellets for thermal energy production: A review of combustion models. *Appl. Energy* **127**, 135–140 (2014).
4. Wang, T. et al. Combustion behavior of refuse-derived fuel produced from sewage sludge and rice husk/wood sawdust using thermogravimetric and mass spectrometric analyses. *J. Clean. Prod.* **222**, 1–11 (2019).
5. Beidaghi Dizaji, H. et al. Generation of high quality biogenic silica by combustion of rice husk and rice straw combined with pre-and post-treatment strategies—A review. *Appl. Sci.* **9**(6), 1083 (2019).
6. Fernandes, I. J. et al. Characterization of rice husk ash produced using different biomass combustion techniques for energy. *Fuel* **165**, 351–359 (2016).
7. Chen, Y. et al. Application studies of activated carbon derived from rice husks produced by chemical-thermal process—A review. *Adv. Colloid Interface Sci.* **163**(1), 39–52 (2011).
8. de Almeida, W. L. et al. Study of structural and optical properties of ZnO nanoparticles synthesized by an eco-friendly tapioca-assisted route. *Mater. Chem. Phys.* **258**, 123926 (2021).
9. Moayedi, H. et al. Applications of rice husk ash as green and sustainable biomass. *J. Clean. Prod.* **237**, 117851 (2019).
10. Fernandes, I. J. et al. Production and characterization of silica materials from rice husk ash by different combustion processes. *Powder Technol.* **436**, 119473 (2024).
11. Azat, S. et al. Sustainable production of pure silica from rice husk waste in Kazakhstan. *J. Clean. Prod.* **217**, 352–359 (2019).
12. Fernandes, I. J. et al. Characterization of silica produced from rice husk ash: Comparison of purification and processing methods. *Mater. Res.* **20**(Suppl 2), 512–518 (2017).
13. Chaikawang, C. et al. Surface modification of rice husk ash as anodes for lithium ion batteries. *Mater. Today Proc.* **5**(6), 13989–13994 (2018).
14. Hossain, S. S., Mathur, L. & Roy, P. Rice husk/rice husk ash as an alternative source of silica in ceramics: A review. *J. Asian Ceram. Soc.* **6**(4), 299–313 (2018).
15. Feng, J., Yamaji, N. & Mitani-Ueno, N. Transport of silicon from roots to panicles in plants. *Proc. Jpn. Acad. Ser. B* **87**(7), 377–385 (2011).
16. Currie, H. A. & Perry, C. C. Silica in plants: Biological, biochemical and chemical studies. *Ann. Bot.* **100**(7), 1383–1389 (2007).
17. Pa, F. C., Abdullah, C. & Fazlul, B. Review of extraction of silica from agricultural wastes using acid leaching treatment. *Adv. Mater. Res.* **626**, 997–1000 (2013).
18. Sankar, S. et al. Rapid sonochemical synthesis of spherical silica nanoparticles derived from brown rice husk. *Ceram. Int.* **44**(7), 8720–8724 (2018).
19. Fernandes, L. et al. Characterization of synthetic amorphous silica (SAS) used in the ceramics industry. *Interceram Int. Ceram. Rev.* **63**, 220–224 (2014).
20. Zemnukhova, L. et al. Biomass derived silica containing products for removal of microorganisms from water. *Int. J. Environ. Sci. Technol.* **12**, 1495–1502 (2015).
21. Pode, R. J. R. Potential applications of rice husk ash waste from rice husk biomass power plant. *Renew. Sustain. Energy Rev.* **53**, 1468–1485 (2016).
22. Worasuwannarak, N. et al. Pyrolysis behaviors of rice straw, rice husk, and corncob by TG-MS technique. *J. Anal. Appl. Pyrol.* **78**(2), 265–271 (2007).
23. Mirmohamadsadeghi, S. & Karimi, K. Recovery of silica from rice straw and husk. Current developments in biotechnology and bioengineering. Elsevier, 411–433 (2020).
24. Eliche-Quesada, D. et al. Characterization and evaluation of rice husk ash and wood ash in sustainable clay matrix bricks. *Ceramics International* **43**(1), 463–475 (2017).
25. Ghafoorian, N. S. et al. Investigation of the effect of rice husk derived Si/SiC on the morphology and thermal stability of carbon composite aerogels. *Mater. Des.* **86**, 279–288 (2015).
26. Mor, S. et al. Nanosilica extraction from processed agricultural residue using green technology. *J. Clean. Prod.* **143**, 1284–1290 (2017).
27. Liao, N. et al. First principle investigation on structural and electronic properties of silicon oxycarbide ceramics. *J. Alloys Compounds* **647**, 665–669 (2015).
28. Athinayaranan, J. et al. Synthesis of biogenic silica nanoparticles from rice husks for biomedical applications. *Ceram. Int.* **41**(1), 275–281 (2015).
29. Marqués, M. et al. A novel crystalline SiCO compound. *Phys. Chem. Chem. Phys.* **17**(38), 25055–25060 (2015).
30. Halimah, M. et al. Study of rice husk silicate effects on the elastic, physical and structural properties of borotellurite glasses. *Mater. Chem. Phys.* **238**, 121891 (2019).
31. Khoshnood Motlagh, E. et al. A comparative study on rice husk and rice straw as bioresources for production of carbonaceous adsorbent and silica. *Biomass Convers. Biorefin.* **12**(12), 5729–5738 (2022).
32. Nandyanto, A., et al. Synthesis of silica particles from rice straw waste using a simple extraction method. in *IOP Conference Series: Materials Science and Engineering*. 2016. IOP Publishing.
33. Lu, P. & Hsieh, Y.-L. Highly pure amorphous silica nano-disks from rice straw. *Powder Technol.* **225**, 149–155 (2012).
34. Kumar, A. et al. Rice straw recycling: A sustainable approach for ensuring environmental quality and economic security. *Pedosphere* **33**(1), 34–48 (2023).
35. Singh, R. & Patel, M. Effective utilization of rice straw in value-added by-products: A systematic review of state of art and future perspectives. *Biomass Bioenergy* **159**, 106411 (2022).
36. Van Soest, P. J. Rice straw, the role of silica and treatments to improve quality. *Anim. Feed Sci. Technol.* **130**(3–4), 137–171 (2006).
37. Zemnukhova, L. et al. Composition and structure of amorphous silica produced from rice husk and straw. *Inorg. Mater.* **50**, 75–81 (2014).
38. Ekwenwa, E. B., Wang, Y. & Roskilly, A. The production of bio-silica from agro-industrial wastes leached and anaerobically digested rice straws. *Bioresour. Technol. Rep.* **22**, 101452 (2023).
39. Taiye, M. A., et al. A review of the use of rice husk silica as a sustainable alternative to traditional silica sources in various applications. *Environ. Prog. Sustain. Energy* **e14451** (2024).
40. Bakar, A. H. A. & Carey, C. J. N. Extraction of silica from rice straw using alkaline hydrolysis pretreatment. in *IOP Conference Series: Materials Science and Engineering*. 2020. IOP Publishing.
41. Bortolotto Teixeira, L. et al. Obtaining biogenic silica from sugarcane bagasse and leaf ash. *Waste Biomass Valoriz.* **12**, 3205–3221 (2021).
42. Falk, G. et al. Synthesis of silica nanoparticles from sugarcane bagasse ash and nano-silicon via magnesiothermic reactions. *Ceram. Int.* **45**(17), 21618–21624 (2019).
43. Zaky, R. et al. Preparation of silica nanoparticles from semi-burned rice straw ash. *Powder Technol.* **185**(1), 31–35 (2008).
44. An, D. et al. A study on the consecutive preparation of silica powders and active carbon from rice husk ash. *Biomass Bioenergy* **35**(3), 1227–1234 (2011).

45. Zhang, D.-D. et al. Preparation and antibacterial activity of mesoporous silica based on rice husk ash. *LWT* **185**, 115145 (2023).
46. Mahalingam, V. & Sivaraju, M. Microwave-assisted sol-gel synthesis of silica nanoparticles using rice husk as a precursor for corrosion protection application. *Silicon* **15**(4), 1967–1975 (2023).
47. Nzereogu, P. et al. Silica extraction from rice husk: Comprehensive review and applications. *Hybrid Adv.* **100111** (2023).
48. Montgomery, D. C. *Design and Analysis of Experiments*. John Wiley & Sons (2017).
49. Box, G. E., Hunter, W. H. & Hunter, S. *Statistics for Experimenters*. Vol. 664. John Wiley and Sons New York (1978).
50. Saleh, M. et al. Fabrication of basalt embedded composite fiber membrane using electrospinning method and response surface methodology. *J. Appl. Polym. Sci.* **138**(25), 50599 (2021).
51. Güven, G., Perendeci, A. & Tanyolac, A. J. Electrochemical treatment of deproteinated whey wastewater and optimization of treatment conditions with response surface methodology. *J. Hazard. Mater.* **157**(1), 69–78 (2008).
52. Costa, J. A. S. & Paranhos, C. M. Systematic evaluation of amorphous silica production from rice husk ashes. *J. Clean. Prod.* **192**, 688–697 (2018).
53. Kongmanklang, C. & Rangsriwatananon, K. Hydrothermal synthesis of high crystalline silicalite from rice husk ash. *J. Spectrosc.* **2015**(1), 696513 (2015).
54. Rafiee, E. et al. Optimization of synthesis and characterization of nanosilica produced from rice husk (a common waste material). *Int. Nano Lett.* **2**, 1–8 (2012).
55. Payá, J. et al. Reuse of industrial and agricultural waste in the fabrication of geopolymeric binders: Mechanical and microstructural behavior. *Materials* **14**(9), 2089 (2021).
56. Prasara-A, J. & Gheewala, S. H. Sustainable utilization of rice husk ash from power plants: A review. *J. Clean. Prod.* **167**, 1020–1028 (2017).
57. Haq, I. U., Akhtar, K. & Malik, A. Effect of experimental variables on the extraction of silica from the rice husk ash. *J. Chem. Soc. Pak.* **36**(3), 382–387 (2014).
58. Kousha, M. et al. Central composite design optimization of Acid Blue 25 dye biosorption using shrimp shell biomass. *J. Mol. Liq.* **207**, 266–273 (2015).
59. Asfaram, A. et al. Removal of basic dye Auramine-O by ZnS: Cu nanoparticles loaded on activated carbon: optimization of parameters using response surface methodology with central composite design. *RSC Adv.* **5**(24), 18438–18450 (2015).
60. Agarwal, S. et al. Rapid adsorption of ternary dye pollutants onto copper (I) oxide nanoparticle loaded on activated carbon: Experimental optimization via response surface methodology. *J. Environ. Chem. Eng.* **4**(2), 1769–1779 (2016).
61. Dashamiri, S. et al. Multi-response optimization of ultrasound assisted competitive adsorption of dyes onto Cu (OH) 2-nanoparticle loaded activated carbon: central composite design. *Ultrason. Sonochem.* **34**, 343–353 (2017).
62. Balamurugan, K. et al. Predicting correlations in abrasive waterjet cutting parameters of Lanthanum phosphate/Yttria composite by response surface methodology. *Measurement* **131**, 309–318 (2019).
63. Tunç, M. S., Yıldız, B. & Taşar, Ş. Removal of paracetamol from aqueous solution by wood sawdust-derived activated carbon: Process optimization using response surface methodology. *Chem. Eng. Commun.* **209**(8), 1130–1150 (2022).
64. Mehralian, M. et al. Activated carbon prepared from pistachio waste for dye adsorption: Experimental and CCD-based design. *Pigment Resin Technol.* **49**(2), 136–144 (2020).
65. El Maguana, Y. et al. Optimization of preparation conditions of activated carbon from walnut cake using response surface methodology. *Moroc. J. Chem.* **6**(1), 92–105 (2018).
66. Taşdemir, R. et al. Optimization of lead (II) adsorption onto cross-linked polycarboxylate-based adsorbent by response surface methodology. *Arab. J. Sci. Eng.* **46**(7), 6287–6301 (2021).
67. Wang, L. et al. Water-soluble Fe 3 O 4 nanoparticles with high solubility for removal of heavy-metal ions from waste water. *Dalton Trans.* **41**(15), 4544–4551 (2012).
68. Zhao, Y.-G. et al. Preparation and characterization of amino-functionalized nano-Fe 3 O 4 magnetic polymer adsorbents for removal of chromium (VI) ions. *J. Mater. Sci.* **45**, 5291–5301 (2010).
69. Kera, N. H. et al. Selective removal of toxic Cr (VI) from aqueous solution by adsorption combined with reduction at a magnetic nanocomposite surface. *J. Colloid Interface Sci.* **503**, 214–228 (2017).
70. Bayuo, J. et al. Modeling and optimization of trivalent arsenic removal from wastewater using activated carbon produced from maize plant biomass: A multivariate experimental design approach. *Biomass Convers. Bioref.* **14**(19), 24809–24832 (2024).
71. Arslan-Alaton, I. et al. Treatment of azo dye production wastewaters using Photo-Fenton-like advanced oxidation processes: Optimization by response surface methodology. *J. Photochem. Photobiol. A Chem.* **202**(2–3), 142–153 (2009).
72. Zhang, Y., Ghaly, A. & Li, B. Physical properties of rice residues as affected by variety and climatic and cultivation conditions in three continents. *Am. J. Appl. Sci.* **9**(11), 1757 (2012).
73. Donahue, C. J. & Rais, E. A. Proximate analysis of coal. *J. Chem. Educ.* **86**(2), 222 (2009).
74. Racerio-Galaraga, D., et al. Proximate analysis in biomass: Standards, applications and key characteristics. *Results Chem.* **101886** (2024).
75. Hosseinpour, S. et al. Estimation of biomass higher heating value (HHV) based on the proximate analysis by using iterative neural network-adapted partial least squares (INNPLS). *Energy* **138**, 473–479 (2017).
76. Srinath, S. & Reddy, G. V. Combustion and emission characteristics of rice husk in a rectangular fluidized bed combustor. in *Proceedings of the 2nd International Conference on Environmental Science and Technology*, Singapore (2011).
77. Fang, M. et al. Experimental study on rice husk combustion in a circulating fluidized bed. *Fuel Process. Technol.* **85**(11), 1273–1282 (2004).
78. Chen, G. et al. Production of amorphous rice husk ash in a 500 kW fluidized bed combustor. *Fuel* **144**, 214–221 (2015).
79. Quispe, I., Navia, R. & Kahhat, R. Life cycle assessment of rice husk as an energy source. A Peruvian case study. *J. Clean. Prod.* **209**, 1235–1244 (2019).
80. Ninduanddee, P. & Kuprianov, V. I. Co-combustion of rice husk pellets and moisturized rice husk in a fluidized-bed combustor using fuel staging at a conventional air supply. *Songklanakarin J. Sci. Technol.* (2018).
81. Singh, R. I. et al. Studies in an atmospheric bubbling fluidized-bed combustor of 10 MW power plant based on rice husk. *Energy Convers. Manag.* **49**(11), 3086–3103 (2008).
82. Pranolo, S. H. et al. Modeling and simulation of a separate line calciner fueled with a mixture of coal and rice husk. *ASEAN J. Chem. Eng.* **10**(1), 27–33 (2010).
83. Blissett, R. et al. Valorisation of rice husks using a TORBED® combustion process. *Fuel Process. Technol.* **159**, 247–255 (2017).
84. Jain, A. et al. Energy and chemicals from rice husk. *Biomass Bioenergy* **7**(1–6), 285–289 (1994).
85. Kwofie, E. & Ngadi, M. J. R. Sustainable energy supply for local rice parboiling in West Africa: The potential of rice husk. *Renew. Sustain. Energy Rev.* **56**, 1409–1418 (2016).
86. Rozainee, M. et al. Fluidized bed combustion of rice husk to produce amorphous siliceous ash. *Energy Sustain. Dev.* **12**(1), 33–42 (2008).
87. Rozainee, M. et al. Computational fluid dynamics modeling of rice husk combustion in a fluidised bed combustor. *Powder Technol.* **203**(2), 331–347 (2010).
88. Obernberger, I. & Thek, G. J. B. Physical characterisation and chemical composition of densified biomass fuels with regard to their combustion behaviour. *Biomass Bioenergy* **27**(6), 653–669 (2004).
89. Paykani, A. et al. Synthesis gas as a fuel for internal combustion engines in transportation. *Prog. Energy Combust. Sci.* **90**, 100995 (2022).

90. Sukarni, S. et al. Potential and properties of marine microalgae *Nannochloropsis oculata* as biomass fuel feedstock. *Int. J. Energy Environ. Eng.* **5**, 279–290 (2014).
91. Sarkar, D., Chapter 3—Fuels and Combustion. *Thermal Power Plant*. 2015, Elsevier: Amsterdam, The Netherlands.
92. ASTM, D.J.A.I.W.C., PA, USA, 3172–89; Standard Practice for Proximate Analysis of Coal and Coke (2002).
93. Gil, M. A. V. et al. Thermal behaviour and kinetics of coal/biomass blends during co-combustion. *Bioresour. Technol.* **101**(14), 5601–5608 (2010).
94. Tillman, D. A. J. B. Biomass cofiring: The technology, the experience, the combustion consequences. *Biomass Bioenergy* **19**(6), 365–384 (2000).
95. Wang, C. et al. Thermogravimetric studies of the behavior of wheat straw with added coal during combustion. *Biomass Bioenergy* **33**(1), 50–56 (2009).
96. Díez, D. et al. Determination of hemicellulose, cellulose, and lignin content in different types of biomasses by thermogravimetric analysis and pseudocomponent kinetic model (TGA-PKM method). *Processes* **8**(9), 1048 (2020).
97. Bakar, R. A., Yahya, R. & Gan, S. N. Production of high purity amorphous silica from rice husk. *Procedia Chem.* **19**, 189–195 (2016).
98. Pantas, P. M. Thermogravimetric analysis of rice husk and coconut pulp for potential biofuel production by flash pyrolysis. *Malays. J. Anal. Sci.* **18**(3), 705–710 (2014).
99. López, R. et al. Thermogravimetric analysis of lignocellulosic and microalgae biomasses and their blends during combustion. *J. Therm. Anal. Calorim.* **114**, 295–305 (2013).
100. Chandrasekhar, S. et al. Review processing, properties and applications of reactive silica from rice husk—An overview. *J. Mater. Sci.* **38**, 3159–3168 (2003).
101. Daffalla, S. B., Mukhtar, H. & Shaharun, M. S. Preparation and characterization of rice husk adsorbents for phenol removal from aqueous systems. *PLoS ONE* **15**(12), e0243540 (2020).
102. Srivastava, V. C., Mall, I. D. & Mishra, I. M. Characterization of mesoporous rice husk ash (RHA) and adsorption kinetics of metal ions from aqueous solution onto RHA. *J. Hazard. Mater.* **134**(1–3), 257–267 (2006).
103. Kaur, P. & Kaur, K. Adsorptive removal of imazethapyr and imazamox from aqueous solution using modified rice husk. *J. Clean. Prod.* **244**, 118699 (2020).
104. Bansal, M. et al. Removal of Cr (VI) from aqueous solutions using pre-consumer processing agricultural waste: A case study of rice husk. *J. Hazard. Mater.* **162**(1), 312–320 (2009).
105. Daffalla, S. B., Mukhtar, H. & Shaharun, M. S. Characterization of adsorbent developed from rice husk: Effect of surface functional group on phenol adsorption (2010).
106. Adam, E., Balakrishnan, S. & Wong, P. L. Rice husk ash silica as a support material for ruthenium based heterogenous catalyst. *J. Phys. Sci.* **17**(2), 1–13 (2006).
107. Le, V. H., Thuc, C. N. H. & Thuc, H. H. Synthesis of silica nanoparticles from Vietnamese rice husk by sol–gel method. *Nanoscale Res. Lett.* **8**, 1–10 (2013).
108. Javed, S. H. et al. Characterization of silica from sodium hydroxide treated rice husk. *J. Pak. Inst. Chem. Eng.* **37**(1), 97–101 (2009).
109. Mušić, S., Filipović-Vinceković, N. & Sekovanić, L. Precipitation of amorphous SiO<sub>2</sub> particles and their properties. *Braz. J. Chem. Eng.* **28**, 89–94 (2011).
110. Ferraro, R. M. et al. Carbon neutral off-white rice husk ash as a partial white cement replacement. *J. Mater. Civ. Eng.* **22**(10), 1078–1083 (2010).
111. Azat, S. et al. Extraction of high-purity silica from rice husk via hydrochloric acid leaching treatment. *Turk. J. Chem.* **43**(5), 1258–1269 (2019).
112. Omatola, K. & Onojah, A. Elemental analysis of rice husk ash using X-ray fluorescence technique (2009).
113. Kurama, H. & Kurama, S. The effect of chemical treatment on the production of active silica from rice husk. In *18th international mining congress and exhibition of Turkey-IMCET* (2003).
114. Mahmud, A. et al. Acid leaching as efficient chemical treatment for rice husk in production of amorphous silica nanoparticles. *ARPN J. Eng. Appl. Sci.* **11**(22), 13384–13388 (2016).
115. Körbahti, B. K. & Tanyolac, A. Electrochemical treatment of simulated textile wastewater with industrial components and Levafix Blue CA reactive dye: Optimization through response surface methodology. *J. Hazard. Mater.* **151**(2–3), 422–431 (2008).
116. Ölmez, T. The optimization of Cr (VI) reduction and removal by electrocoagulation using response surface methodology. *J. Hazard. Mater.* **162**(2–3), 1371–1378 (2009).
117. Joglekar, A. & May, A. Product excellence through design of experiments. *Cereal Foods World* **32**(12), 857 (1987).
118. Deb, A., Debnath, A. & Saha, B. Ultrasound-aided rapid and enhanced adsorption of anionic dyes from binary dye matrix onto novel hematite/polyaniline nanocomposite: Response surface methodology optimization. *Appl. Organomet. Chem.* **34**(2), e5353 (2020).
119. Myers, R. H. J. P. Response Surface Methodology (RSM). 489–492 (2002).
120. Gun, M. et al. Optimization of silica extraction from rice husk using response surface methodology and adsorption of safranin dye. *Int. J. Environ. Res.* **16**(2), 20 (2022).
121. Thakur, M. et al. Process optimization for the production of cellulose nanocrystals from rice straw derived  $\alpha$ -cellulose. *Mater. Sci. Energy Technol.* **3**, 328–334 (2020).
122. Jamaluddin, A. et al. Response surface methodology approaches in producing amorphous silica from rice straw ash. *Construction* **3**(2), 196–206 (2023).

## Acknowledgements

The authors acknowledged Bahir Dar Institute of Technology, Bahir Dar University, Ethiopia for supporting the laboratory facilities.

## Author contributions

YTZ, HJK, AAT and AYF: Designed the experiments, collected and analysed the data, interpretation of results, and wrote the original draft. AAA, AKS, FAG and TDT: designed the experiments, and Editing. WWK, TAW, and MTM performed characterization (TG/DT, XRF, BET) tests. TAY: conceptualization, supervised, statistical analysis, editing and reviewed the paper.

## Declarations

### Competing interests

The authors declare no competing interests.

### Additional information

Correspondence and requests for materials should be addressed to T.A.Y.

Reprints and permissions information is available at [www.nature.com/reprints](http://www.nature.com/reprints).

**Publisher's note** Springer Nature remains neutral with regard to jurisdictional claims in published maps and institutional affiliations.

**Open Access** This article is licensed under a Creative Commons Attribution-NonCommercial-NoDerivatives 4.0 International License, which permits any non-commercial use, sharing, distribution and reproduction in any medium or format, as long as you give appropriate credit to the original author(s) and the source, provide a link to the Creative Commons licence, and indicate if you modified the licensed material. You do not have permission under this licence to share adapted material derived from this article or parts of it. The images or other third party material in this article are included in the article's Creative Commons licence, unless indicated otherwise in a credit line to the material. If material is not included in the article's Creative Commons licence and your intended use is not permitted by statutory regulation or exceeds the permitted use, you will need to obtain permission directly from the copyright holder. To view a copy of this licence, visit <http://creativecommons.org/licenses/by-nc-nd/4.0/>.

© The Author(s) 2024